ELSEVIER

Journal of Chromatography A, 746 (1996) 185–198

JOURNAL OF CHROMATOGRAPHY A

Characterization of protein adsorption by composite silica–polyacrylamide gel anion exchangers II. Mass transfer in packed columns and predictability of breakthrough behavior

M. Aurora Fernandez[1], W. Scott Laughinghouse, Giorgio Carta*

Center for Bioprocess Development, Department of Chemical Engineering, University of Virginia, Charlottesville, VA 22903-2442, USA

Received 1 December 1995; revised 10 April 1996; accepted 11 April 1996

Abstract

Rates of uptake of proteins by a composite silica–polyacrylamide gel ion exchanger known as Q-HyperD are obtained for hydrodynamic conditions identical to those found in a chromatographic column operated at a high mobile phase velocity by means of a shallow bed technique. Under conditions of intraparticle mass transfer control, mass transfer rates in the shallow bed were the same as those measured when the sorbent particles were suspended in an agitated vessel, indicating that the intraparticle mass transfer rate is independent of the hydrodynamic conditions outside the particle and consistent with a purely diffusional transport mechanism. The predictability of breakthrough curves based on kinetic parameters obtained from batch experiments is assessed by comparing experimental results for different proteins with predictions of a model which incorporates the external film resistance and intraparticle diffusion. This model is in excellent agreement with the experimental results even at extremely high mobile phase velocities. Very large dynamic capacities are obtained with columns packed with Q-HyperD media as a result of their high static capacity, rapid uptake kinetics and mechanical strength that prevents compression of the particles even at elevated flow-rates.

Keywords: Mass transfer; Preparative chromatography; Ion exchangers; Breakthrough curves; Stationary phases, LC; Proteins; Albumin; Ovalbumin; Lactalbumin

1. Introduction

In Part I of this series, [J. Chromatogr. A, 646 (1996) 169] we have described the equilibrium and sorption kinetics of proteins for a composite silica–polyacrylamide gel ion exchanger, known under the trade name HyperD [1]. The unique structure of this sorbent comprises two parts: a rigid porous polystyrene–silica composite support particle and a functionalized polyacrylamide hydrogel that fills its pores. The porous support provides mechanical strength while the hydrogel provides a large sorption capacity for proteins.

One of the applications of the HyperD media is its use as a high capacity stationary phase for frontal

*Corresponding author

[1]Current address: Departamento de Ingegneria Quimica, Universidad de Oviedo, Spain.

0021-9673/96/$15.00
PII S0021-9673(96)00338-X

chromatography to recover and purify proteins in dilute solutions. A key performance parameter in such applications is the column dynamic binding capacity (DBC) [2]. This parameter can be evaluated experimentally by continuously feeding a given protein solution to the packed column at a certain flow-rate until the eluent concentration reaches a target percentage of the feed concentration, typically 10%. The column dynamic capacity can be defined as the amount of protein supplied to the column to this point divided by the column volume [3]. If one continues to feed the protein solution to the column, a breakthrough curve is obtained. In ion-exchange columns, the dynamic capacity and the shape of the breakthrough curve are in general affected by many factors, including the adsorption isotherm, extraparticle and intraparticle mass transfer resistance, and by any deviations from perfect plug flow in the column [4]. In general the dynamic capacity decreases with mobile phase velocity.

Models for the prediction of breakthrough curves for adsorption beds are reviewed in detail in [4]. In principle, if parameters that characterize intraparticle kinetic mechanisms are known experimentally, then it should be possible to predict the breakthrough behavior of a packed column. Such methods have been applied to ion-exchange columns for protein separations by several authors. Tsou and Graham [5], for example, obtained breakthrough curves for bovine serum albumin (BSA) in a column packed with the soft-gel ion exchanger Sephadex A-50. They compared experimental results with breakthrough curves obtained via computer simulations which incorporated a two-film mass transfer model with the assumption that equilibrium in the column is described by the Langmuir isotherm. They found that the breakthrough curve was essentially determined by the external film mass transfer resistance and by the equilibrium isotherm and that an approximate theoretical prediction could be obtained estimating the film thickness from empirical correlations for mass transfer coefficients in adsorption beds. However, they found that the breakthrough curve could not be predicted a priori since an equilibrium capacity much smaller than the static adsorption capacity determined in independent batch experiments was needed to yield a good match of the experimental results even for a mobile phase velocity of only about 46 cm/h. According to these authors, the observed reduction in capacity was due to the compressibility of the stationary phase which resulted in a restriction of the accessibility of some of the ion-exchange groups.

The predictability of breakthrough curves of proteins in columns packed with S-Sepharose using parameters derived from batch kinetic experiments has been discussed by Skidmore et al. [6]. This polysaccharide-based ion exchanger is not as soft as the one used by Tsou and Graham, and these authors were able to use a higher mobile phase velocity of about 76 cm/h. Skidmore et al. used two models to predict their breakthrough curves: the first assuming empirically a reaction-controlled kinetics and the second assuming a more realistic control by external film and pore diffusional limitations. The intraparticle kinetic parameters of each model were fitted from batch data and the remaining ones were estimated from correlations. When this was done for lysozyme and BSA, either model provided an excellent prediction of the breakthrough curve for the smaller lysozyme molecule but only approximate predictions for the breakthrough curve of BSA. In general, however, a satisfactory agreement between experimental results and model predictions was found for the initial breakthrough of protein.

Modeling of breakthrough curves of proteins has also been discussed for the case of rigid, silica-based, porous ion-exchange packings by Kopaciewicz et al. [7]. The compressibility of the stationary phase is not significant in this case and the authors were able to use velocities as high as 700 cm/h with 10-μm particles. They found an inverse relation of the dynamic capacity of BSA with particle size and flow-rate of the mobile phase and a direct relation with pore size. Thus, they suggested that for proteins such as BSA, large pores (1000 Å) are needed to obtain dynamic capacities near the static capacity of the stationary phase at high mobile phase velocities. On the other hand, for smaller proteins such as α-lactalbumin, they found that, except for relatively large particles, the dynamic capacity was essentially independent of pore size, particle size and mobile phase velocity over a broad range. These authors also modeled the breakthrough behavior taking into

account mass transfer limitations. They found that the breakthrough curve of α-lactalbumin with a mobile phase velocity of 360 cm/h could be modeled accurately, but that only an approximate description was possible for BSA.

In Part I of this series, we obtained equilibrium isotherms, representing the static adsorption capacity and mass transfer rates in an agitated contactor for three representative proteins in Q-HyperD media with different particle sizes. We found that the uptake isotherms could be described empirically either by the Langmuir isotherm or by the mass action law for heterovalent exchange. Mass transfer rates could be modeled by taking into account the external resistance in the hydrodynamic boundary layer surrounding the particle with a film mass transfer coefficient and the intraparticle resistance with a diffusion model. The corresponding equilibrium and kinetic parameters could be valid also when the particles are packed in a column operated at elevated mobile phase flow-rates. However, this is not always the case. For example, when dealing with stationary phases which lack adequate mechanical strength, the particles may be compressed during the packing process or by pressure generated by the frictional resistance at high flows, making both equilibrium and kinetics different from what one finds in agitated contactors. Differences could also occur when dealing with particles which are permeable to fluid flow, such as those used for perfusion chromatography [8]. When such particles are suspended in an agitated vessel, intraparticle mass transfer must occur primarily by diffusion mechanisms. However, when such particles are packed in a column operated under appropriate conditions [9–13], intraparticle convection can be dominant. In this case, intraparticle mass transfer would be much faster in a packed column than in an agitated vessel and strongly dependent on the flow-rate of the mobile phase. For this situation, a prediction of breakthrough curves solely on the basis of the mass transfer kinetics obtained in an agitated contactor would be unreliable.

Thus, in this work we have experimentally determined the adsorption kinetics of proteins with Q-HyperD media for conditions which are identical to those prevailing in a chromatographic column for a broad range of mobile phase velocities. The predictability of breakthrough curves from data obtained for these conditions was also assessed by comparing experimental breakthrough curves with model predictions.

2. Experimental

2.1. Materials

Samples of Q-HyperD-F and Q-HyperD-M (Lot. No. 3259 and 3186) were obtained from BioSepra (Marlborough, MA, USA). The samples were pretreated as described in Part I. The particle size distribution of each sample was also determined experimentally (see Part I). The volume average particle diameters were 49 μm and 76 μm for the F and M grades of Q-HyperD.

BSA, ovalbumin and α-lactalbumin were obtained from Sigma (St. Louis, MO, USA) as purified preparations. Experiments were carried out in 50 m*M* Tris–HCl buffer solutions at pH 8.5–8.6. At this pH, each of the proteins is strongly negatively charged and is very favorably adsorbed by Q-HyperD media at low ionic strengths. Equilibrium isotherms at 23±2°C are given in Part I for each protein.

2.2. Uptake kinetics

A "shallow bed" apparatus was assembled to determine in a direct way the rate of uptake of the proteins by Q-HyperD for hydrodynamic conditions identical to those that would be found in a chromatographic column separated at a high mobile phase flow-rate. The apparatus is shown schematically in Fig. 1 and is a modification of the classic shallow bed technique developed by Boyd et al. [14] to determine ion-exchange kinetics. Various modifications of this shallow bed technique have been used by different authors to determine mass transfer in ion-exchange sorbents. For example, Saunders et al. [15] and Jones and Carta [16] used a recirculated shallow bed apparatus to determine the batch uptake kinetics of amino acids by ion-exchange resins, while Yoshida et al. [17] used a semibatch shallow bed technique to determine the uptake kinetics of BSA by strongly basic chitosan ion exchangers. The

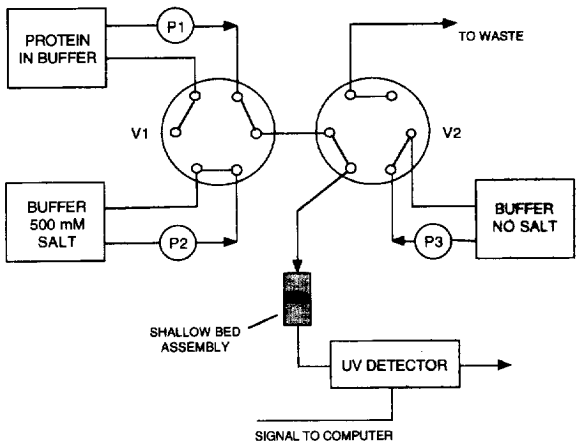

Fig. 1. Shallow bed apparatus. P1, P2 and P3 are HPLC pumps. V1 and V2 are six-port switching valves.

apparatus used in this work comprises a shallow bed assembly that was constructed by packing a small sample of Q-HyperD media between two layers of S-HyperD media of the same particle size grade in a 0.3 cm diameter, 1.2 cm long stainless steel column. The column was machined from a stainless steel rod and fitted with Omnifit end caps with 0.5-μm frits at each end.

Samples of S-HyperD-F and S-HyperD-M were obtained from BioSepra. These stationary phases have a structure analogous to that of Q-HyperD. They are manufactured from the same silica support particles, but they contain a hydrogel with a cation-exchange functionality. In a 50 m*M* Tris–HCl buffer at pH 8.5–8.6, S-HyperD is totally inert with respect to BSA, which is negatively charged at this pH. From batch experiments and from experiments in chromatography columns packed with S-HyperD, we determined that there is no uptake of BSA by this media for these conditions. Hence, the S-HyperD layers in the shallow bed assembly serve only to provide mechanical support. We also determined the particle size distribution and average particle size of the samples of S-HyperD-F and S-HyperD-M and found them to be essentially the same as those of the corresponding grades of Q-HyperD. Thus, the shallow bed assemblies constructed in this manner allow one to determine the uptake kinetics of BSA by Q-HyperD particles for the same hydrodynamic conditions that would be found in an identical column packed only with Q-HyperD. However, since the Q-HyperD layer is very thin, provided that the flow of mobile phase is sufficiently high, each of the Q-HyperD particles is exposed to essentially the same solution concentration. Hence, the driving force for the uptake process is known exactly which simplifies the comparison of experimental mass transfer rates with kinetic models.

The shallow bed apparatus also comprises three Waters (Milford, MA, USA; Model 510) HPLC pumps, a Waters (Model 484) tunable absorbance detector and a set of two 6-port valves (Valco, Houston, TX, USA; Model C6U) connected as sketched in Fig. 1. The setup allows a very rapid switching of streams to the shallow bed. A run consists of letting the protein solution flow through the shallow bed for a set period of time. After this time, a buffer solution containing no salt is fed to the shallow bed to remove quickly any unabsorbed protein from the packing interstices and from the connecting lines. Since the adsorption is extremely favorable, essentially none of the adsorbed BSA is removed during this phase. Then, the flow is switched to a buffer solution containing 500 m*M* NaCl. At this salt concentration, all of the BSA adsorbed on the Q-HyperD media contained in the shallow bed assembly is removed (see Part I) yielding a "chromatographic" peak as depicted in Fig. 2. The amount of protein adsorbed during the time of contact with the protein solution is calculated from the area of the peak obtained upon salt elution

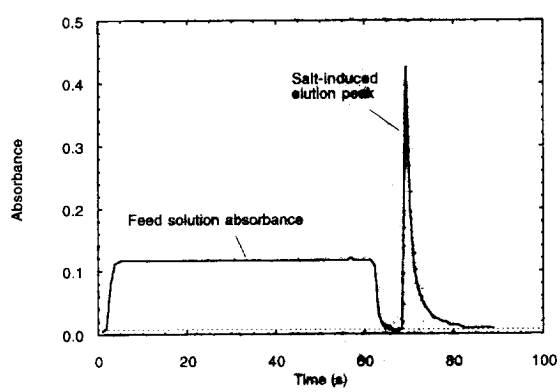

Fig. 2. Typical detector trace for a Q-HyperD-F shallow bed adsorption run with BSA at $u = 5940$ cm/h and $C_F = 0.25$ mg/cm^3.

in conjunction with a calibration curve. The shallow bed is then reequilibrated with the buffer solution and readied for a new run involving a different time of contact with the feed protein solution. The detector wavelength was set at 280 nm.

In packing the shallow bed assembly, a layer of S-HyperD, approximately 0.5 cm deep, was pipetted into the column as a slurry of approximately 50% concentration while applying a suction at the opposite end with a syringe connected to the fritted outlet connector. A small Q-HyperD sample was then introduced, also as a 50% slurry, using a 10 mm^3 pipette. Since the slurry concentration was not known exactly, the amount of Q-HyperD media introduced in the column could not be determined accurately by direct measurement. Thus, it was determined by comparing the maximum amount of protein adsorbed by the shallow bed after a long time of contact, with the static equilibrium capacity determined independently in batch experiments (see Part I). The volume of Q-HyperD media (particles only) calculated in this way was found to be about $3 \cdot 10^{-3}$ cm^3 and varied only slightly for the different shallow bed columns packed. This figure is consistent with the volume of slurry introduced. The column was then filled to the top with an additional layer of S-HyperD and capped with the fritted inlet connector.

2.3. Breakthrough behavior

Breakthrough curves were obtained for 10 cm× 0.3 I.D. glass columns (Omni Microbore Column; Omnifit, Toms River, NJ, USA) equipped with 0.5-μm stainless steel frits and Omnifit connectors. Samples of Q-HyperD-F and Q-HyperD-M were pipetted into these columns as a 50% slurry while applying a slight suction at the opposite end with a syringe. After packing, each column was run with a buffer flow-rate of about 9 cm^3/min for several column volumes. The level of media in the column dropped by about 0.5 cm during this phase. Thus, the top connector was removed and additional media pipetted in to completely fill the column while withdrawing buffer at the opposite end. The top cap was then reconnected and the media level rechecked again after running several column volumes at 9 cm^3/min. After the initial packing, each column appeared to be visually stable during the course of this study.

The extraparticle void fraction of the HyperD columns was estimated by packing similar columns with the same technique and determining the total mass of media plus buffer in each column from weight measurements. Since the density of the hydrated particles can be estimated (see Part I), knowing the weight of media plus buffer in the column allows one to calculate the extraparticle void fraction. The volume of each column was also determined by weighing each column empty and filled with water. The void fraction determined in this manner for columns packed with Q-HyperD-F and M was 0.49 and 0.48, respectively.

Each column was used in the same set-up designed for the shallow bed experiments. To record breakthrough curves, the column effluent was run through the UV detector operated at 280 nm. The output mV signal of this detector was collected with a microcomputer-based data acquisition system. The effluent protein concentration was then obtained from the digitized signal through appropriate calibration curves. Flow-rates were varied between about 0.5 cm^3/min and 9 cm^3/min, corresponding to bed superficial velocities in the range 400 to 7200 cm/h. Protein feed solutions in concentrations of 1 and 2 mg/cm^3 in 50 m*M* Tris–HCl buffer at pH 8.5–8.6 were used. After each breakthrough experiment, the column was rinsed with 50 m*M* Tris–HCl buffer, regenerated with a 500 m*M* NaCl and then rinsed again with buffer.

3. Results and discussion

3.1. Shallow bed uptake kinetics

In Part I of this series we showed that the batch uptake kinetics of proteins by Q-HyperD suspended in an agitated vessel can be described accurately by taking into account the external film mass transfer resistance and intraparticle diffusion. We also showed that, when the selectivity is very high as in the case of protein uptake at low salt concentrations, the relative importance of these two resistances in

series is determined in an approximate way by the magnitude of the parameter

$$\delta = \frac{1}{5}\frac{k_f R_p}{D_s}\frac{C_0}{q_0} \quad (1)$$

relative to unity. In this equation k_f is the external mass transfer coefficient, R_p is the particle radius, D_s is the intraparticle diffusivity, C_0 is the solution concentration and q_0 is the saturation capacity of the sorbent. Since the equilibrium uptake of proteins by Q-HyperD is very favorable, the saturation capacity, q_0, is essentially constant. Thus, for a given protein, δ varies primarily only with the value of the film mass transfer coefficient and with the protein concentration in solution.

If the intraparticle transport mechanism in HyperD is independent of the hydrodynamic conditions outside the particles, as would be the case for a diffusional transport mechanism, the same kinetic model and parameters obtained in stirred batch experiments should apply to the shallow bed experiments. The only differences would be that in the shallow bed experiments, the solution concentration remains constant and equal to the feed concentration and that a different external film mass transfer coefficient would apply for each hydrodynamic condition. The latter, of course, depends on the thickness of the hydrodynamic boundary layer that surrounds the particle, which in turn is a function of the mobile phase velocity. The criterion expressed by Eq. (1) should also apply, provided that C_0 is set equal to the feed protein concentration, C_F. In stirred batch experiments we found that for BSA in both Q-HyperD-F and M, the uptake process was essentially controlled by the intraparticle resistance ($\delta > 1$) when $C_0 = 2$ mg/cm^3.

Since k_f is likely to be larger in a packed-bed operated with a high superficial velocity than in an agitated contactor, it is apparent that at the same protein concentration intraparticle mass transfer would be controlling also in the shallow bed apparatus. Thus, for these conditions, experiments in the two types of contactors should be directly comparable.

Experimental results for the uptake of BSA by Q-HyperD-F and M for a protein concentration of 2 mg/cm^3 are shown in Fig. 3 and Fig. 4. In these figures, the shallow bed data are compared with those obtained when the sorbents were suspended in an agitated vessel and with the model developed in Part I for the latter conditions. In each case, the amount adsorbed at a particular time is normalized with the saturation capacity value, q_0. The shallow bed data are shown at mobile phase velocities of 2550, 4240 and 5940 cm/h. For these conditions, there is clearly no effect of the mobile phase velocity on the rates of uptake of BSA by Q-HyperD-F and Q-HyperD-M and these rates are essentially the same as those found in the agitated contactor. Moreover, it

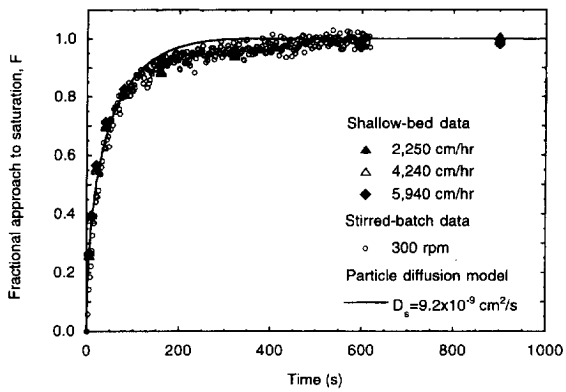

Fig. 3. Transient uptake of BSA by Q-HyperD-F in a stirred batch with $C_0 = 2$ mg/cm^3 and in a shallow bed contactor at different mobile phase velocities with $C_F = 2$ mg/cm^3. The line is calculated from the particle diffusion model with $D_s = 9.2 \cdot 10^{-9}$ cm^2/s.

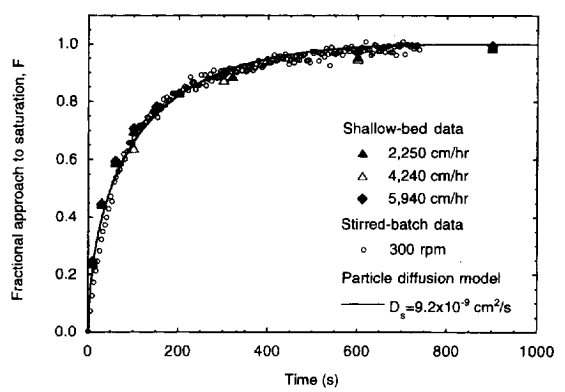

Fig. 4. Transient uptake of BSA by Q-HyperD-M in a stirred batch with $C_0 = 2$ mg/cm^3 and in a shallow bed contactor at different mobile phase velocities with $C_F = 2$ mg/cm^3. The line is calculated from the particle diffusion model with $D_s = 9.2 \cdot 10^{-9}$ cm^2/s.

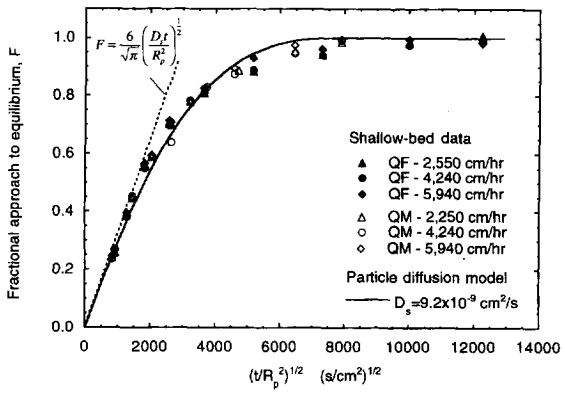

Fig. 5. Transient uptake of BSA by Q-HyperD-F ($R_p = 2.45 \cdot 10^{-3}$ cm) and Q-HyperD-M ($R_p = 3.80 \cdot 10^{-3}$ cm) in the shallow bed contractor at superficial velocities of 2550, 4240 and 5940 cm/h with $C_F = 2$ mg/cm^3 plotted as a function of $\sqrt{t/R_p^2}$. The line is calculated from the particle diffusion model with $D_s = 9.2 \cdot 10^{-9}$ cm^2/s.

appears that the shallow bed data are consistent with diffusion theory also when particles of different size are compared. Fig. 5 shows the shallow bed data for Q-HyperD-F and Q-HyperD-M at the different superficial velocities tested with $C_F = 2$ mg/cm^3 plotted as a function of $\sqrt{t/R_p^2}$ as suggested by classical Fickian diffusion models [18]. Clearly, the data for the two different size grades of Q-HyperD are coincident when plotted in this form, as it is expected for diffusive transport in the particles. Thus, we conclude that the intraparticle mass transfer mechanism in Q-HyperD is completely independent of the hydrodynamic conditions outside the particles and of a purely diffusive nature.

In Part I of this paper, we showed that intraparticle mass transfer in Q-HyperD can be described by a model which assumes a pseudo-homogeneous diffusion of protein molecules which interact electrostatically with the media functionality. A value of the effective intraparticle diffusivity $D_s = 9.2 \cdot 10^{-9}$ cm^2/s was found to fit the batch data for both Q-HyperD-F and M. Lines calculated from this model (Eq. 9 or Eq. 10 in Part I) with the same value of D_s are shown in Figs. 3–5. Clearly, the same diffusivity value provides an excellent fit of these shallow bed data for a protein concentration of 2 mg/cm^3 from low to high values of the fractional approach to saturation. As shown in Fig. 5, at low values of F, the data converge to the asymptotic limit [18]

$$F = \frac{6}{\sqrt{\pi}} \left(\frac{D_s t}{R_p^2} \right)^{1/2} \tag{2}$$

which represents the well known theoretical limit for diffusive transport in spherical particles with a constant surface concentration.

Conditions where the external film resistance should be dominant over a significant portion of the uptake curve were also studied in the shallow bed apparatus. Such conditions can be found by selecting a protein concentration sufficiently low to make δ significantly smaller than unity. For these conditions, since the fluid phase concentration is constant in the shallow bed, for relatively short contact times the uptake curve should be linear and described by the equation

$$\text{Amount adsorbed} = \bar{q} V_M = \frac{3 k_f}{R_p} V_M C_F t \tag{3}$$

where V_M is the volume of sorbent and t the time of contact with the protein solution. Note that $3/R_p$ is the external surface area of the particles per unit particle volume. Since the left hand side is known experimentally, k_f can be obtained for each mobile phase velocity by comparing Eq. (3) with the initial linear rate of protein uptake at a suitably low protein concentration. It should be noted, however, that even for these conditions, Eq. (3) would break down for long times of contact. In this case, in fact, the

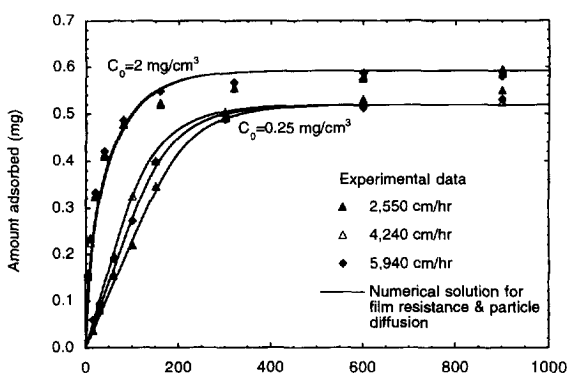

Fig. 6. Transient uptake of BSA by Q-HyperD-F in the shallow bed apparatus at low and high protein concentrations. Lines are calculated from the numerical solution of the complete kinetic model including external film and intraparticle diffusional resistances.

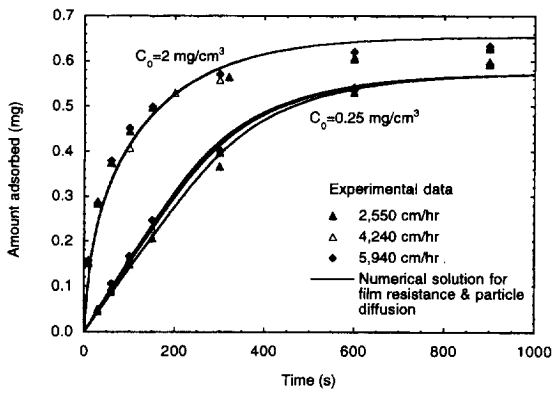

Fig. 7. Transient uptake of BSA by Q-HyperD-M in the shallow bed apparatus at low and high protein concentrations. Lines are calculated from the numerical solution of the complete kinetic model including external film and intraparticle diffusional resistances.

sorbent particles would approach saturation and the intraparticle resistance would become dominant again.

Experimental uptake data for Q-HyperD-F and -M in the shallow bed apparatus are shown in Fig. 6 and Fig. 7 respectively, comparing a protein concentration of 0.25 mg/cm^3 with the data for 2 mg/cm^3. At the lower concentration, there appears to be some dependence of uptake on the mobile phase flow-rate although the same final saturation capacity is obtained. This behavior, of course, would be expected if the external mass transfer resistance is indeed controlling for short times, since the mass transfer coefficient, k_f, is an increasing function of the mobile phase velocity, The k_f values obtained by fitting the initial slope of these curves with Eq. (3) are summarized in Table 1. In each case, k_f increases with flow-rate, while the values for the smaller Q-HyperD-F are larger than those for the bigger size Q-HyperD-M particles.

With these fitted k_f values and with the previously determined value of the intraparticle diffusivity D_s, it should now be possible to predict the entire uptake behavior in the shallow bed apparatus. To do this, the complete kinetic model, including both the external film resistance and intraparticle diffusion must be solved in conjunction with the adsorption isotherm. The corresponding equations are

$$\frac{\partial q}{\partial t} = \frac{D_s}{r^2}\frac{\partial}{\partial r}\left(r^2\frac{\partial q}{\partial r}\right) \tag{4}$$

$$r = 0, \quad \frac{\partial q}{\partial r} = 0 \tag{4a}$$

$$r = R_p, \quad D_s\frac{\partial q}{\partial r} = k_f(C_F - C_i) \tag{4b}$$

$$t = 0, \quad q = 0 \tag{4c}$$

where r is the radial particle coordinate, q is the solute concentration in the particles, and C_i is the solution concentration at the particle surface. This is related to $q(R_p)$ via the equilibrium isotherm which is given by Eq. 4b in Part I.

A numerical solution of these equations was obtained as described in Part I of this paper using $D_s = 9.2\cdot10^{-9}$ cm^2/s, the experimental k_f values given in Table 1 and the equilibrium parameters given in Part I. The amount adsorbed at each time was calculated from

$$\bar{q}V_M = \frac{3V_M}{R_p^3}\int_0^{R_p} r^2 q(r,t)dr \tag{5}$$

and the results are shown in Figs. 6 and 7. There is a

Table 1
External film mass transfer coefficients for the uptake of BSA by Q-HyperD media in a 50 m*M* Tris–HCl buffer at pH 8.6 in the shallow bed contactor

Media	u (cm/h)	$Re = ud_p/\epsilon\nu$	$(k_f)_{exp}$ (cm/s)	$(k_f)^{(a)}_{est}$ (cm/s)
Q-HyperD-F	2550	0.70	$2.7\cdot10^{-3}$	$3.0\cdot10^{-3}$
	4240	1.16	$3.3\cdot10^{-3}$	$3.9\cdot10^{-3}$
	5940	1.62	$4.0\cdot10^{-3}$	$4.6\cdot10^{-3}$
Q-HyperD-M	2550	1.06	$2.3\cdot10^{-3}$	$2.4\cdot10^{-3}$
	4240	1.80	$2.5\cdot10^{-3}$	$3.1\cdot10^{-3}$
	5940	2.50	$2.6\cdot10^{-3}$	$3.7\cdot10^{-3}$

[a] Values estimated from Eq. (6).

Table 2
Calculated values of δ for BSA in the shallow bed experiments with different protein concentrations based on $D_s = 9.2 \cdot 10^{-9}$ cm^2/s and $q_0 = 200$ mg/cm^3

Media	u (cm/h)	C_F (mg/cm^3)	δ
Q-HyperD-F	2550	2.0	1.5
	2550	0.25	0.18
	4240	2.0	1.8
	4240	0.25	0.22
	5940	2.0	2.1
	5940	0.25	0.27
Q-HyperD-M	2550	2.0	1.9
	2550	0.25	0.24
	4240	2.0	2.1
	4240	0.25	0.26
	5940	2.0	2.2
	5940	0.25	0.27

substantial agreement with the experimental data. For the low protein concentration, the complete kinetic model predicts the observed dependence of the uptake rate on the mobile phase flow-rate for each particle size, consistent with the fact that k_f increases with mobile phase velocity. At the high concentration, however, this dependence on flow-rate disappears. For these conditions, the numerical solution is essentially coincident with the solution for intraparticle mass transfer control with a rectangular isotherm that was shown in Figs. 3 and 4, indicating that intraparticle diffusion is indeed limiting. Conversely, at 0.25 mg/cm^3, the external resistance is initially dominant and remains so for a significant range of times. This can also be seen by considering the δ values calculated for each of the experimental conditions as summarized in Table 2. Clearly, $\delta < 1$, indicating that the external film resistance is important, when $C_F = 0.25$ mg/cm^3 and $\delta > 1$, indicating that the external resistance is not significant, when $C_F = 2$ mg/cm^3.

Mass transfer coefficients in packed bed can also be estimated approximately using literature correlations. We have used a correlation originally developed by Carberry [19] to test the validity of a priori predictions of k_f for Q-HyperD. The mass transfer coefficient is given by

$$k_f = 1.15 \frac{u}{\epsilon} (Re)^{-1/2} (Sc)^{-2/3} \quad (6)$$

where ϵ is the extraparticle void fraction, $Re = ud_p/\epsilon\nu$ and $Sc = \nu/D$. ν is the kinematic viscosity of the mobile phase. This correlation has been verified experimentally in shallow beds for ion-exchange systems with small Reynolds numbers [20]. k_f values calculated with this equation are given in Table 1. A value of $\epsilon = 0.5$ was used in the calculations, consistent with the void fraction determined for chromatographic columns packed with Q-HyperD. As seen in Table 1, experimental and estimated values of k_f are quite close for Q-HyperD-F. Some disagreement is seen for the Q-HyperD-M data. On the other hand, the external resistance is less significant for those bigger particles, so that a less accurate estimation of k_f should generally suffice for predictive purposes.

3.2. Breakthrough behavior

Experimental breakthrough curves at different mobile phase velocities are shown in Fig. 8a and b for BSA and ovalbumin in 2 mg/cm^3 feed concentrations with the Q-HyperD-F column. Similar

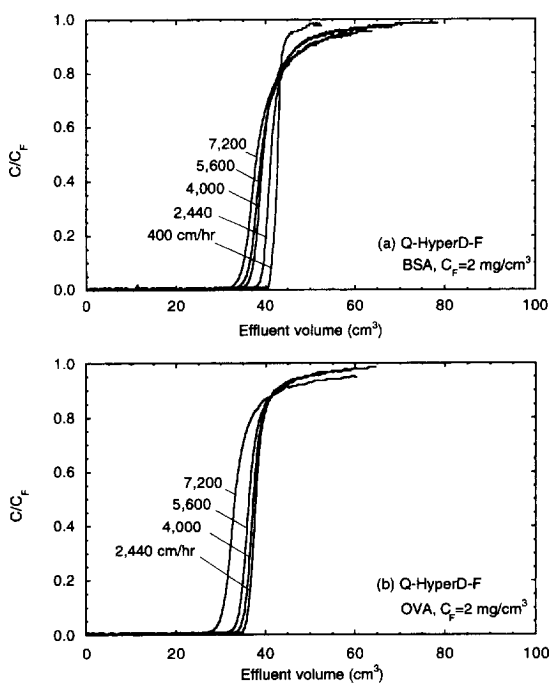

Fig. 8. Experimental breakthrough curves for (a) BSA and (b) ovalbumin for a Q-HyperD-F column at different mobile phase velocities with $C_F = 2$ mg/cm^3.

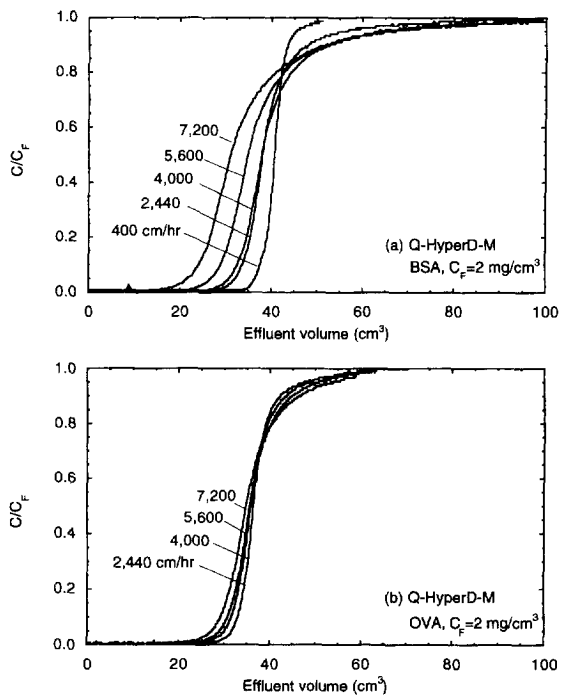

Fig. 9. Experimental breakthrough curves for (a) BSA and (b) ovalbumin for a Q-HyperD-M column at different mobile phase velocities with $C_F = 2$ mg/cm^3.

results for the Q-HyperD-M column are given in Fig. 9, while Fig. 10 shows breakthrough curves for α-lactalbumin in 1 mg/cm^3 concentration for the Q-HyperD-M column. In all cases, the volume at which breakthrough occurs and the slope of the profile are reduced as the mobile phase superficial

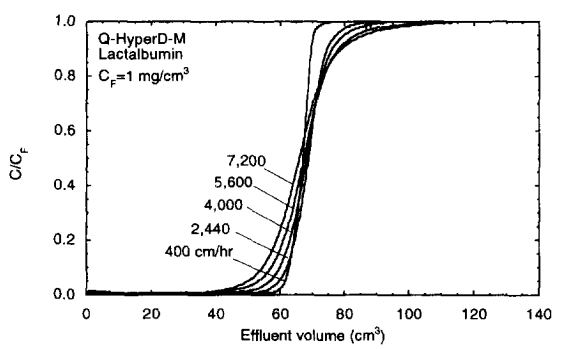

Fig. 10. Experimental breakthrough curves for α-lactalbumin for a Q-HyperD-M column at different mobile phase velocities with $C_F = 1$ mg/cm^3.

velocity is increased. Thus, for these runs the column dynamic capacity decreases with flow-rate.

The shape of the breakthrough curves is determined by the equilibrium isotherm, by mass transfer resistances and by possible deviations from plug flow. In general, a numerical solution is needed for an exact prediction of the effects of each contribution. On the other hand, for certain limiting forms of the isotherm, such as linear or rectangular, analytic expressions for the breakthrough curve can be found [21]. Vermeulen [22], for example, has demonstrated that for favorable monovalent ion-exchange or adsorption systems, breakthrough curves can be adequately predicted by assuming that the equilibrium isotherm is rectangular, when the true equilibrium constant is greater than 5. Yoshida et al. [21] have obtained a corresponding criterion for the case of heterovalent ion-exchange systems, by comparing the exact numerical solution of a model that includes intraparticle diffusion and external film mass transfer resistance with an approximate solution for a rectangular isotherm. Their kinetic model is essentially the same as that which we have found describes the uptake behavior of Q-HyperD. However, for their approximate analytical solution, Yoshida et al. used the linear driving force approximation to describe intraparticle mass transfer, instead of the particle dilution equation. Under constant pattern conditions, their analytic solution is given by

$$\frac{C}{C_F} = \frac{1}{\delta}\exp\left(\tau - \xi + \delta - 1 - \frac{1}{\delta}\right)$$

$$\text{for } \tau - \xi \leq -\delta + 1 + \frac{1}{\delta} - \ln\left(\frac{1+\delta}{\delta}\right) \qquad (7)$$

$$\frac{C}{C_F} = 1 - \frac{\delta}{1+\delta}\exp\left\{\left[-\tau + \xi - \delta + 1 + \frac{1}{\delta} - \ln\left(\frac{1+\delta}{\delta}\right)\right]\Big/\delta\right\}$$

$$\text{for } \tau - \xi \geq -\delta + 1 + \frac{1}{\delta} - \ln\left(\frac{1+\delta}{\delta}\right) \qquad (7a)$$

when $\delta \geq 1$, and by

$$\frac{C}{C_F} = \exp(\tau - \xi - 1)$$

$$\text{for } \tau - \xi \leq 1 - \ln(1+\delta) \qquad (8)$$

$$\frac{C}{C_F} = 1 - \frac{\delta}{1+\delta}\exp\{[-\tau + \xi + 1 - \ln(1+\delta)]/\delta\}$$

$$\text{for } \tau - \xi \geq 1 - \ln(1+\delta) \tag{8a}$$

when $\delta \geq 1$. In these equations,

$$\delta = \frac{1}{5}\frac{k_f R_p}{D_s}\frac{C_F}{q_0} \tag{9}$$

$$\tau = \frac{3k_f}{R_p}\frac{C_F}{q_0}\left(t - \frac{\epsilon L}{u}\right) \tag{10}$$

$$\xi = \frac{3(1-\epsilon)}{R_p}\frac{k_f L}{u} \tag{11}$$

Following Yoshida et al., the rectangular isotherm approximation for the heterovalent exchange of a species with effective charge n with a univalent counterion is valid when

$$K' = K\left(\frac{q_R}{C_S}\right)^{n-1} \geq 100 \tag{12}$$

where K is the equilibrium constant for the exchange reaction, q_R is the total ion concentration in the stationary phase and C_s is the total ion concentration in solution. Values of K and q_R can be obtained from the data in Part I of this paper. From these data, for a 50 mM Tris–HCl buffer we can calculate that the K' values for the proteins studied are well in excess of 30 000, indicating that the rectangular isotherm approximation is valid. For such conditions, Eqs. (7,8) can be used when $0 \leq \delta \leq 5$ [21].

To test the predictability of the breakthrough behavior of Q-HyperD columns with these equations, we have carried out calculations with Eqs. (7,8) using the D_s values obtained from stirred batch experiments and the film mass transfer coefficients estimated from Eq. (5) for the different proteins and mobile phase velocities. The saturation capacity, q_0, was obtained by numerical integration of the experimental breakthrough curves obtained at the lowest superficial velocity. The resulting values were very close to the values determined independently from batch equilibrium experiments (see Part I). Using the estimated extraparticle void fraction of 0.5, the maximum error was ±6.7% or less. Experimental and predicted breakthrough curves with a mobile phase velocity of 4000 cm/h are given in Fig. 11, Fig. 12 and Fig. 13 for BSA and ovalbumin with Q-HyperD-F and M with a feed concentration of 2 mg/cm^3 and for α-lactalbumin with Q-HyperD-M for a feed concentration of 1 mg/cm^3. The agreement is excellent in all cases, especially in view of the fact that there is no adjustable parameter in these calculations. The values of δ are between 1.1 and 2.2 for the experimental conditions tested. Yoshida et al. have shown that only when $\delta > 10$ is the breakthrough curve not affected by the external film resistance. The relatively small δ values obtained in our work indicate that there is a significant effect of the external film resistance on the breakthrough behavior of Q-HyperD. This effect is felt particularly in the initial portion of the breakthrough curve. Neglecting it would lead to error in the prediction of the breakthrough profile in this region.

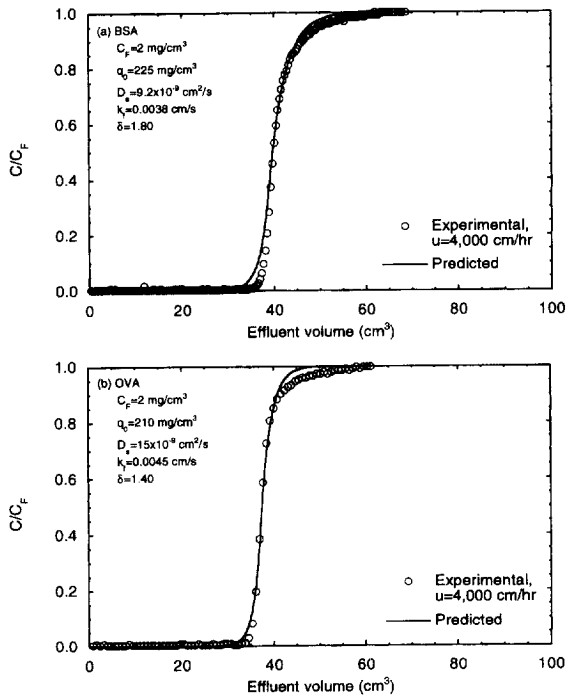

Fig. 11. Comparison of experimental and predicted breakthrough curves for (a) BSA and (b) ovalbumin for a Q-HyperD-F column with a mobile phase velocity of 4000 cm/h. $C_F = 2$ mg/cm^3.

The column dynamic capacity at 10% breakthrough was also calculated for each of the experimental runs and from the model, Eqs. (7,8). The results are shown in Fig. 14 and Fig. 15. In accordance with the experimental behavior, the model

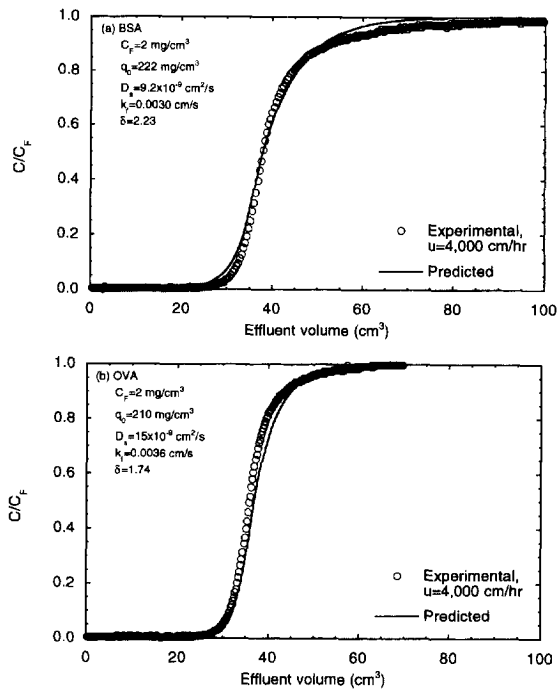

Fig. 12. Comparison of experimental and predicted breakthrough curves for (a) BSA and (b) ovalbumin for a Q-HyperD-M column with a mobile phase velocity of 4000 cm/h. $C_F = 2$ mg/cm^3.

predicts a reduction in the dynamic capacity as the mobile phase velocity is increased. However, even in the worst case (BSA with Q-HyperD-M) the dynamic capacity remains very large and greater than 60% of the static capacity when the column is operated at the extremely large mobile phase velocity of 7200 cm/h.

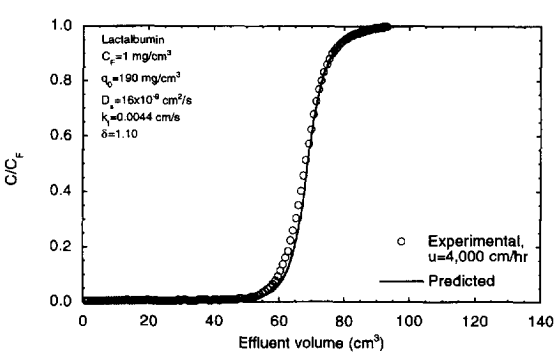

Fig. 13. Comparison of experimental and predicted breakthrough curves for α-lactalbumin for a Q-HyperD-M column with a mobile phase velocity of 4000 cm/h. $C_F = 1$ mg/cm^3.

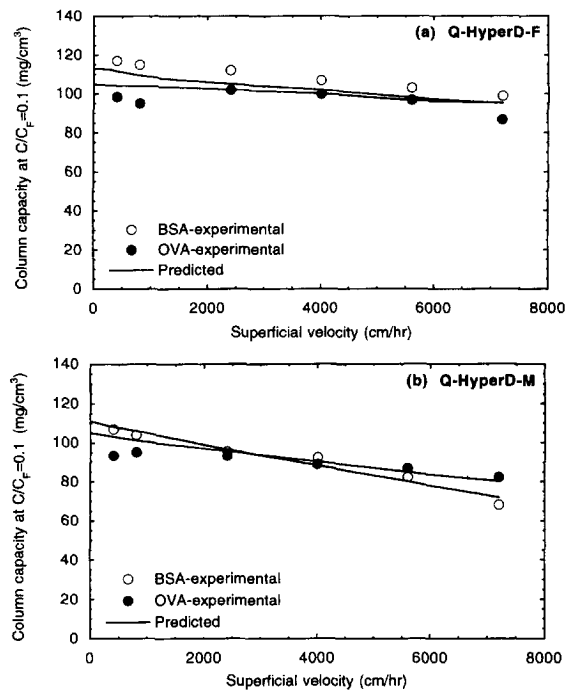

Fig. 14. Comparison of experimental and predicted column dynamic capacity at 10% breakthrough for BSA and ovalbumin for (a) Q-HyperD-F and (b) Q-HyperD-M columns as a function of the mobile phase velocity. $C_F = 2$ mg/cm^3.

4. Conclusions

We have determined that the intraparticle mass transfer of proteins in Q-HyperD media is unaffected by the hydrodynamic conditions outside the particles. Hence, for conditions where the intraparticle mass

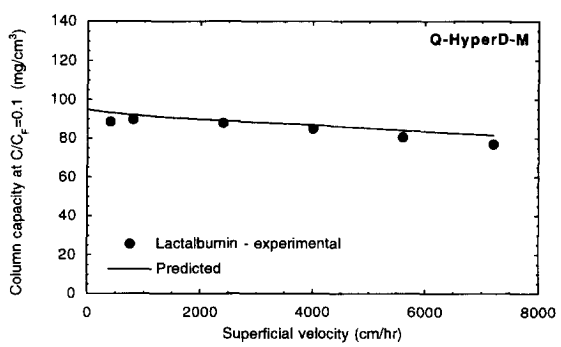

Fig. 15. Comparison of experimental and predicted column dynamic capacity at 10% breakthrough for α-lactalbumin for a Q-HyperD-M column as a function of the mobile phase velocity. $C_F = 1$ mg/cm^3.

transfer resistance is controlling, mass transfer rates in HyperD are independent of the particular type of contacting apparatus (e.g. stirred batch, packed bed, fluidized bed) in which they are used. Experimentally, we found that mass transfer rates were the same when HyperD was suspended in an agitated contactor or packed in a chromatographic column.

In a recent article, Rodrigues et al. [23] have studied the breakthrough behavior of BSA for a 0.5 cm diameter, 10 cm long column packed with Q-HyperD media which was reported to have a particle diameter of 35 μm. These authors obtained breakthrough curves which exhibited little dependence on flow-rate and a dynamic capacity that decreased only slightly when the mobile phase superficial velocity was changed from about 611 cm/h to about 2445 cm/h. They asserted that this behavior is a consequence of intraparticle convection and likened the behavior of Q-HyperD to that of Poros Q/M (PerSeptive Biosystems, Cambridge, MA, USA), a chromatography medium for which they noted that intraparticle mass transfer is convection-dominated. Contrary to their conclusions, however, we have found no evidence that intraparticle convection plays any role in the performance of Q-HyperD. In fact, if intraparticle convection were dominant, intraparticle mass transfer rates would increase with the mobile phase velocity for the laminar flow conditions of a liquid chromatography column [8–13]. In contrast, we have found that intraparticle mass transfer rates in Q-HyperD are independent of flow and the same whether the particles are suspended in an agitated contactor, where intraparticle convection cannot occur to a significant extent even for extremely permeable particles, or they are packed in a shallow bed contactor operated at elevated flow-rates, where intraparticle convection would occur if it were possible in these particles. If intraparticle convection occurred in Q-HyperD, as suggested by Rodrigues et al., it would be strongly dependent on the mobile phase velocity and would yield mass transfer rates much larger in a packed bed than in an agitated contactor. The lack of this dependence and the close agreement of agitated contactor and shallow bed contactor data clearly indicate that intraparticle mass transfer of proteins in Q-HyperD is of a purely diffusive nature. In fact, consistent with diffusion theory, intraparticle mass transfer rates in Q-HyperD vary in inverse proportion with the square of the particle size and decrease with the size of the diffusing solute.

We have also assessed the predictability of the breakthrough behavior of Q-HyperD columns by comparing experimental results with the predictions of a model which incorporates external and intraparticle mass transfer resistances, using parameters determined form batch experiments and estimates from literature correlations. We found that the model predictions were in excellent agreement with the experimental data even at extremely high mobile phase velocities. Thus, deviations from plug flow are apparently not significant for these conditions.

The model could also accurately predict the dynamic capacity for different proteins as a function of the mobile phase velocity. Remarkably, Q-HyperD afforded an exceptionally high dynamic capacity even at elevated flow-rates. In the worst case (BSA with Q-HyperD-M), the column retained a dynamic capacity in excess of 70 mg/cm^3 when operated at a 7200 cm/h. In a better case, with the smaller Q-HyperD-F media, the dynamic capacity for BSA was in excess of 100 mg/cm^3 at 7200 cm/h. Q-HyperD-F and M owe this exceptional performance to their extremely high static capacity, their rapid uptake kinetics and their mechanical strength that allows operation at extremely high flow-rates without apparent compression. The rapid uptake kinetics exhibited by HyperD is due to the large driving force for diffusion provided by its high sorption capacity and the resulting diffusion of electrostatically interacting protein in the hydrogel. Thus, its unique morphology appears to combine in a successful way the advantages of soft-gel matrices with those of rigid supports to yield a robust stationary phase suitable for high speed separation and purification of proteins.

5. Symbols

C_F feed protein concentration
C_i solution concentration of protein at particle surface
C_0 initial protein concentration in solution
C_s total ion concentration in solution
d_p particle diameter
D solution diffusivity
D_e effective diffusivity

D_s intraparticle diffusivity
F fractional approach to saturation
K equilibrium constant for heterovalent exchange
K' modified equilibrium constant, Eq. (12)
k_f external film mass transfer coefficient
L column length
n effective charge of protein
q protein concentration in adsorbent based on particle volume
$\bar{q}$ average protein concentration in sorbent particles
q_0 sorbent saturation capacity based on particle volume
q_R total ion concentration in adsorbent based on particle volume
r radial particle coordinate
Re Reynolds number ($=ud_p/\epsilon\nu$)
R_p particle radius
Sc Schmidt number (ν/D)
t time
u superficial velocity
V_M volume of sorbent
δ parameter defined by Eq. (1) or Eq. (9)
ν kinematic viscosity
ϵ extraparticle void fraction
τ dimensionless time, Eq. (10)
ξ parameter defined by Eq. (11)

Acknowledgments

This work was supported in part by BioSepra, Inc. M.A.F. is grateful for the support by FIYCT of Asturias, Spain. G.C. is indebted to S. Kessler for insightful discussions.

References

[1] E. Boschetti, J. Chromatogr. A, 658 (1994) 207.
[2] H.A. Chase, J. Chromatogr., 297 (1984) 179.
[3] A.M. Tsai, D. Englert and E.E. Graham, J. Chromatogr., 504 (1990) 89.
[4] T. Vermeulen, M.D. LeVan, N.K. Hiester and G. Klein, Adsorption and Ion-Exchange, in R.H. Perry, D.W. Green and J.O. Maloney (Editors), Perry's Chemical Engineers' Handbook, 6th ed., Section 16, McGraw-Hill, New York, 1986.
[5] H.-S. Tsou and E.E. Graham, AIChE J., 31 (1985) 1959.
[6] G.L. Skidmore, B.J. Horstmann and H.A. Chase, J. Chromatogr., 498 (1990) 113.
[7] W. Kopaciewicz, S. Fulton and S.Y. Lee, J. Chromatogr., 409 (1987) 111.
[8] N.B. Afeyan, N.F. Gordon, I. Mazsaroff, L. Varady, S.P. Fulton, Y.B. Yang and F.E. Regnier, J. Chromatogr., 519 (1990) 1.
[9] A.E. Rodrigues, Z.P. Lu and J.M. Loureiro, Chem. Eng. Sci., 107 (1991) 2765.
[10] G. Carta, M. Gregory, D.J. Kirwan and H. Massaldi, Sep. Technol., 2 (1992) 273.
[11] A.I. Liapis and M.A. McCoy, J. Chromatogr., 599 (1992) 87.
[12] D. Frei, E. Schweinheim and Cs. Horváth, Biotechnol. Progr., 9 (1993) 273.
[13] R. Freitag, D. Frey and Cs. Horváth, J. Chromatogr. A, 686 (1994) 165.
[14] G.E. Boyd, A.W. Adamson and L.S. Myers, J. Am. Chem. Soc., 69 (1947) 2836.
[15] M.S. Saunders, J.B. Vierow and G. Carta, AIChE J., 35 (1989) 53.
[16] I.L. Jones and G. Carta, Ind. Eng. Chem. Res., 32 (1993) 117.
[17] H. Yoshida, M. Yoshikawa and T. Kataoka, AIChE J., 40 (1994) 2034.
[18] D.M. Ruthven, Principles of Adsorption and Adsorption Processes, Wiley, New York, 1984, pp. 166–181.
[19] J.J. Carberry, AIChE J., 6 (1960) 460.
[20] T. Kataoka, N. Sato and K. Ueyama, J. Chem. Eng. Jpn., 1 (1968) 38.
[21] H. Yoshida, T. Kataoka and D.M. Ruthven, Chem. Eng. Sci., 39 (1984) 1489.
[22] T. Vermeulen, Ind. Eng. Chem., 45 (1953) 1664.
[23] A.E. Rodrigues, J.M. Loureiro, C. Chenou and M. Rendueles de la Vega, J. Chromatogr. B, 664 (1995) 233.